

1 **Multi-source data fusion of optical satellite imagery to characterize habitat selection**  
2 **from wildlife tracking data**

3 Vanessa Brum-Bastos <sup>1</sup>, Jed Long <sup>2</sup>, Katharyn Church <sup>1</sup>, Greg Robson <sup>1,3</sup>, Rogério de Paula <sup>4</sup>,  
4 Urška Demšar <sup>1</sup>

5  
6 <sup>1</sup> School of Geography & Sustainable Development, University of St Andrews, Irvine  
7 Building, North Street, St Andrews, KY16 9AL, UK; {vdsbb, kgc, gsr3, urska.demsar}@st-  
8 andrews.ac.uk

9 <sup>2</sup> Department of Geography, Western University, Social Science Centre Rm 2322, London,  
10 ON, Canada; jlong83@uwo.ca

11 <sup>3</sup> Department of Geography and Planning, Queen's University, Mackintosh-Corry Hall, Room  
12 E208, Kingston, ON, Canada

13 <sup>4</sup> Centro Nacional de Pesquisa e Conservação de Mamíferos Carnívoros, ICMBIO, Estr.  
14 Hisaichi Take Bayashi, 8600 - Usina, Atibaia, Brazil; rogerio.paula@icmbio.gov.br

15  
16 \* Correspondence: vdsbb@st-andrews.ac.uk

17 **Declarations of interest:** none

18 **Abstract**

19 Wildlife tracking data allow monitoring of how organisms respond to spatio-temporal changes  
20 in resource availability. Remote sensing data can be used to quantify and qualify these  
21 variations to understand how movement is related to these changes. The use of remote sensing  
22 data with concurrent high levels of spatial and temporal detail may hold potential to improve  
23 our understanding of habitat selection. However, no current orbital sensor produces data with  
24 simultaneous high temporal and high spatial resolution, therefore alternative methods are  
25 required to generate remote sensing data that matches the high spatial-temporal resolution of

26 modern wildlife tracking data. We present an analytical framework, not yet used in movement  
27 ecology, for data fusion of optical remote sensing data from multiple satellites and wildlife  
28 tracking data to study the impact of seasonal vegetation patterns on the movement of maned  
29 wolves (*Chrysocyon brachyurus*). We use multi-source data fusion to combine MODIS data  
30 with higher spatial resolution data (ASTER, Landsat 4-5-7-8, CBERS 2-2B) and create a  
31 synthetic NDVI product with a 15 m spatial detail and daily temporal resolution. We also use  
32 the higher spatial resolution data to create a multi-source NDVI product with same level of  
33 spatial detail but coarser temporal resolution and data from MODIS to create a single-source  
34 NDVI product with high temporal resolution but coarse spatial resolution. We combine the  
35 three different spatial-temporal resolution NDVI products with GPS tracking data of maned  
36 wolves to create step-selection functions (SSF), which are models used in ecology to investigate  
37 and predict habitat selection by animals. The SSF model based on multi-source NDVI had the  
38 best performance predicting the probability of use of visited locations given its NDVI value.  
39 The SSF based on the raw MODIS NDVI product, one which is commonly employed by  
40 ecologists, had the poorest performance for our study species. These findings indicate that, in  
41 contrast with current practice in movement ecology, a detailed spatial resolution of contextual  
42 environmental variable may be more important than a detailed temporal resolution, when  
43 investigating wildlife habitat selection regarding vegetation, although this result will be highly  
44 dependent on species. The choice of data set should therefore take into account not only the  
45 scale of movement but also the spatial and temporal scales at which dynamic environmental  
46 variables are changing.

47

48

49 **Keywords:** movement analysis, remote sensing, NDVI, MODIS, Landsat, data fusion, multi-  
50 source.

## 51 **1. Introduction**

52 Technological advances in GPS (Global Positioning Systems) have recently made it possible  
53 to collect movement data from animals at an unprecedented level of spatio-temporal detail  
54 (Demšar *et al.*, 2015). At the same time, Earth observation data are increasing in availability  
55 and quality (*e.g.*, at various spatio-temporal resolutions over the last four decades (Neumann *et*  
56 *al.*, 2015)) and can be used to quantify and qualify the context associated with movement  
57 (Dodge *et al.*, 2013). Movement data can be used to monitor changes in behaviour by organisms  
58 adapting to spatio-temporal variations in resource availability. Remote sensing data can be used  
59 to understand how movement is associated with these variations.

60 In the last fifteen years many studies have demonstrated the potential of remotely sensed  
61 indicators for researching animal movement (Kerr and Ostrovsky, 2003; Turner *et al.*, 2003;  
62 Pettorelli *et al.*, 2011). Remotely sensed data has been used to understand zebra migration  
63 (Bartlam-Brooks *et al.*, 2013), waterfowl movement (Henry, Ament and Cumming, 2015) and  
64 human movement context (Brum-Bastos, Long and Demšar, 2018). Surface temperature  
65 retrieved by satellites have been used to explore foraging strategies of albatrosses (Kappes *et*  
66 *al.*, 2015) and investigating the habitat use of sharks (Howey *et al.*, 2017).

67 Amongst all remotely sensed data, NDVI (Normalized Difference Vegetation Index) is one of  
68 the most widely used to contextualize movement, particularly for understanding the effects of  
69 vegetation on wildlife movement (Pettorelli *et al.*, 2011). NDVI is a proxy for the content and  
70 state of the live green vegetation (Rouse *et al.*, 1973) and one of the most successfully used  
71 remote sensing products in movement research (Pettorelli *et al.*, 2011). NDVI is often used to  
72 assess the primary productivity distribution of an area, which has been shown to correlate with

73 behaviour of several species (Pettorelli *et al.*, 2011). It has been successfully combined with  
74 movement data of many species for varied purposes, such as understanding long-distance bird  
75 migration (Thorup *et al.*, 2017), exploring the movement of waterfowl in arid landscapes  
76 (Henry, Ament and Cumming, 2015), studying the effects of environment on the movement of  
77 monkeys and birds (Buchin *et al.*, 2015) and investigating the effects of vegetation productivity  
78 on roe deer performance (Pettorelli *et al.*, 2006). However, almost all of these studies only use  
79 remotely sensed data from a single source, which can lead to high uncertainties in either spatial  
80 or temporal dimension of the context of movement, particularly for studies lasting months or  
81 years.

82 A single satellite source can provide NDVI data with either high spatial resolution or high  
83 temporal resolution. For example, sensors providing daily data have spatial resolutions varying  
84 between 250 - 5000 m. On the other hand, sensors providing higher spatial resolution data (0.5  
85 - 30 m), have temporal resolutions between 15 days and several months, which is temporally  
86 much coarser than most wildlife tracking data. This trade-off means that either the spatial or  
87 temporal resolution component will often be prioritized when linking environmental to  
88 movement data (Neumann *et al.*, 2015), which can be problematic for certain types of  
89 movement behaviour analysis.

90 We propose that the use of remote sensing data with concurrent high level of spatial and  
91 temporal detail has potential to improve our understanding of movement behaviour. To date,  
92 most studies linking wildlife tracking data with Earth observation data use only a single-source  
93 of satellite data (Bühne and Pettorelli, 2017). Alternative methods are therefore required to  
94 develop new remote sensing products for movement analysis, specifically methods that match  
95 the spatial and temporal scales of Earth observation products to those required to link movement  
96 processes with changes in the environment at the scale that both makes sense from data point  
97 of view and biological context. In particular, multi-source data fusion methods, which

98 systematically combine remote sensing data from multiple sensors to capitalize on their  
99 complementary characteristics (Wald, 1999), offer a substantial opportunity for developing new  
100 lines of analysis and answering increasingly complex questions at the intersection of wildlife  
101 movement and environmental change. These methods have only recently been applied  
102 movement ecology (Berman *et al.*, 2019) and are not widely known or used.

103 In this work, we propose a methodology for data fusion of multi-source optical satellite imagery  
104 and tracking data to investigate movement patterns of a specific animal species. We evaluate  
105 three different approaches for calculating NDVI (Normalized Difference Vegetation Index) at  
106 different spatial and temporal resolutions and combine these products with wildlife tracking  
107 data. Specifically, we hypothesize that by fusing high spatial and temporal resolution Earth  
108 observation data, we will be able to better predict the movement and habitat selection of wildlife  
109 species that respond dynamically to environmental conditions. We used data from seven  
110 different sensors to create a synthetic daily and spatially detailed NDVI series with high  
111 temporal and spatial detail (the Multi-source data Fusion product, MF-NDVI), NDVI from  
112 MODIS with high temporal and low spatial resolution (the Single Source product, SS-NDVI),  
113 and NDVI data from ASTER, Landsat 4-5-7-8 and CBERS 2-2B, with low temporal and high  
114 spatial resolution (the Multi-Source product, MS-NDVI). We demonstrate the use of our  
115 proposed methodology on a case study of maned wolves (*Chrysocyon brachyurus*) in the  
116 Brazilian Cerrado to investigate habitat selection relative to primary productivity across the  
117 landscape (defined by NDVI). We used Step-Selection Functions (SSFs), which are a common  
118 approach for studying habitat selection from wildlife tracking data (Thurfjell, Ciuti and Boyce,  
119 2014) to test the relationship between NDVI and habitat selection by maned wolves.

120 The rest of the paper is structured as follows: First we describe related work on movement  
121 contextualization with remote sensing data and provide a description of the biology of our case  
122 study species. In section 3 we describe the data, the Multi-Source (MS), the Single Source (SS),

123 and the Multi-source data Fusion (MF) approaches and explain how we link wildlife tracking  
124 data to the resulting NDVI data sets to compare their performance. This is followed by results.  
125 We conclude with a discussion on how advanced remote sensing techniques such as our new  
126 methodology could improve spatial analysis of wildlife movement.

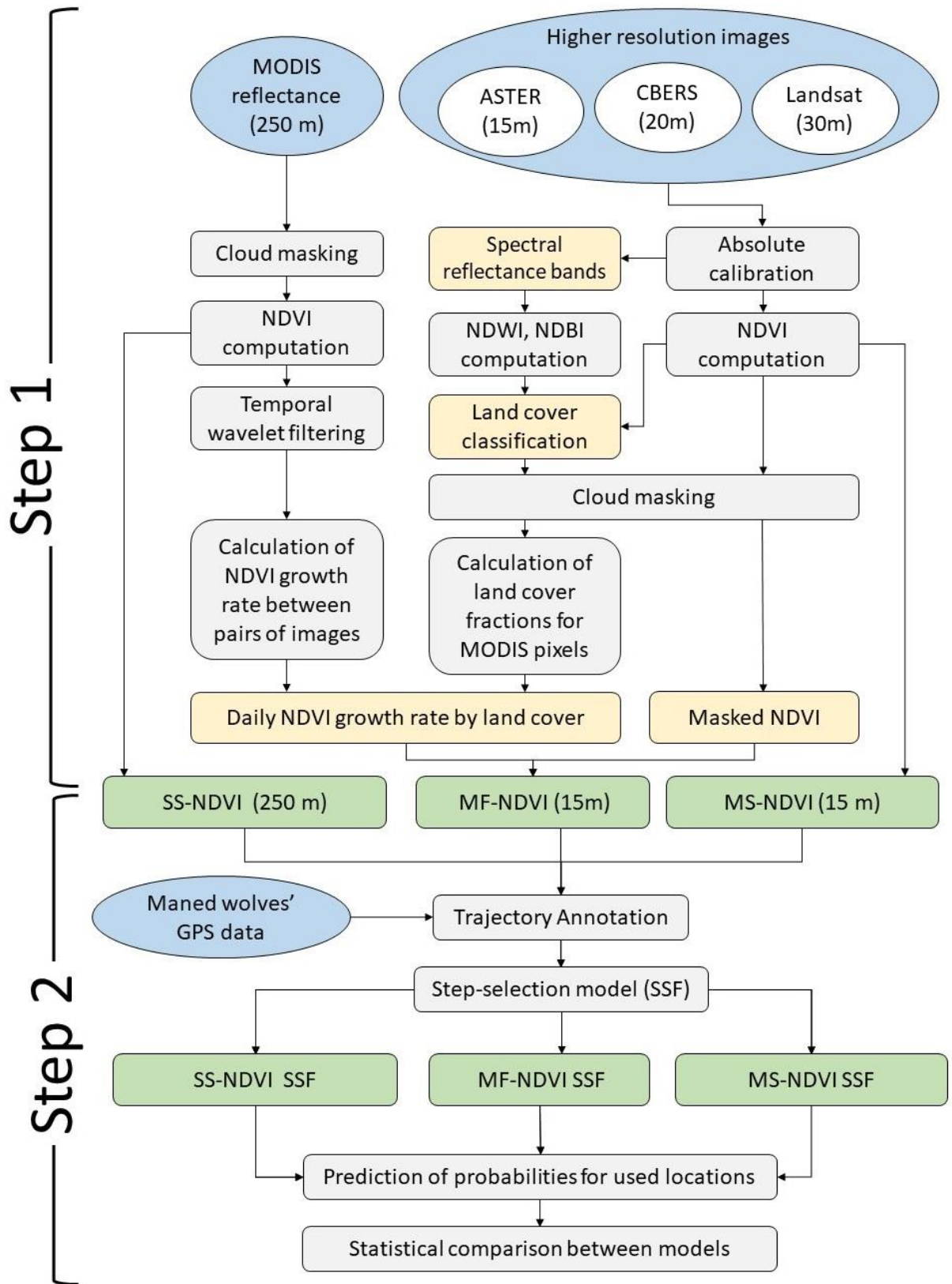
## 127 **2. Methods**

128 We propose and test three methodologies to produce contextual data on vegetation for  
129 movement analysis (Figure 2).

130 In Step 1, we create three NDVI products at three different levels of resolution: a Multi-Source  
131 product (MS), a Single Source (SS) product, and a Multi-Source Data Fusion product (MF).  
132 For this we acquired and fuse high spatial resolution images from seven sensors (MS) and daily  
133 MODIS NDVI (250 m) (SS) to produce daily NDVI data at a higher spatial granularity (15m -  
134 30 m) (MF). We create the MF-NDVI by adapting the method proposed by (Rao *et al.*, 2015),  
135 in which multi-temporal MODIS NDVI, higher resolution NDVI and land cover classification  
136 are used to obtain a NDVI temporal series with high spatial detail.

137 In Step 2, we use the three NDVI products to annotate maned wolves' GPS tracking data and  
138 create Step-Selection Function (SSF) models to evaluate the suitability of each NDVI dataset  
139 for predicting habitat selection of used areas in regard to vegetation greenness. In the rest of  
140 this section we describe the data, the MS and MF approaches and finally how we linked NDVI  
141 data sets to movement data using SSFs to evaluate their use for movement analysis.

142

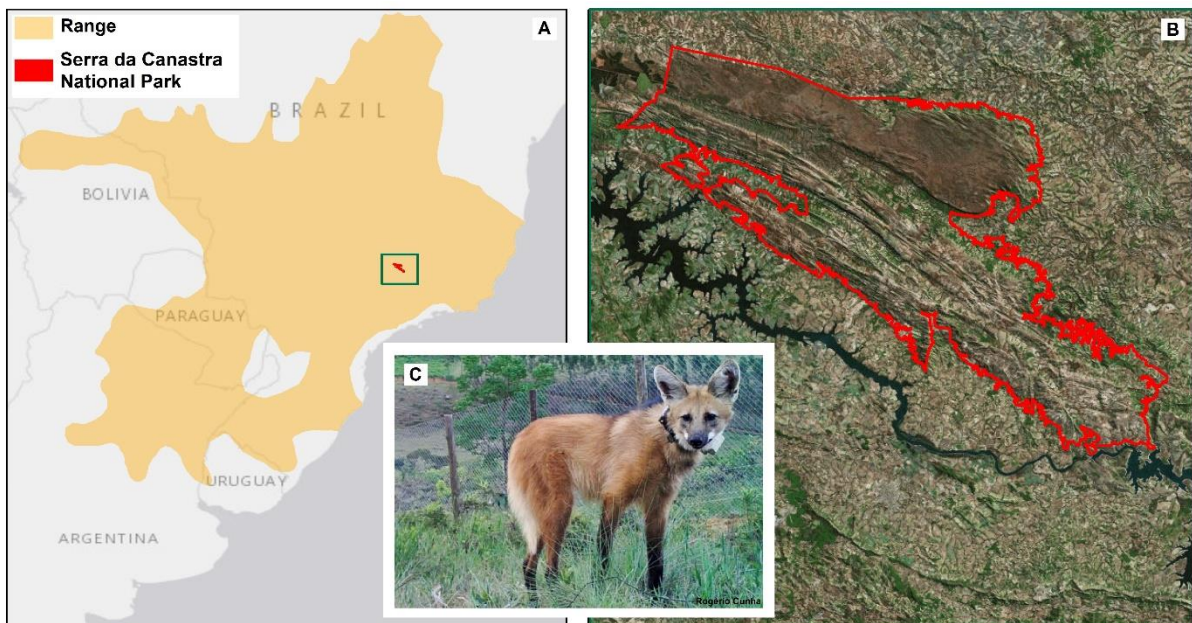


143

144 Figure 2 - The overview of our framework for producing and testing the performance of SS-,  
 145 MF-, and MS NDVI for context-aware movement analysis of maned wolves' tracking data. Step  
 146 1 shows how each of the NDVI data sets were produced and Step 2 shows how tracking data  
 147 were linked to NDVI data sets for performance assessment through Step-Selection Functions.  
 148 Blue ellipses show inputs, grey rectangles show processing steps, yellow rectangles are  
 149 secondary outputs and green rectangles show primary outputs, i.e., the final products.

## 150 2.1. Study Area and Species

151 Maned wolves (*Chrysocyon brachyurus*) are the largest South American canid (de Paula and  
 152 Desbiez, 2014) and are savannah-adapted omnivores found south of the Amazon Forest. Their  
 153 range extends from Bolivia into eastern Brazil, through northern Argentina and Uruguay, to  
 154 central Paraguay (Deem and Emmons, 2005) (Figure 1A). Considered "vulnerable" until 1996  
 155 by IUCN (International Union for Conservation of Nature), the species is currently classified  
 156 as "near threatened" (de Paula and DeMatteo, 2015) and "vulnerable" by the Brazilian  
 157 environmental authorities (ICMBio, 2016).



158  
 159 Figure 1 - A) The range of the maned wolf (*Chrysocyon brachyurus*) in South America. B)



160 Borders of Serra da Canastra National Park (CNP) in Minas Gerais state in Brazil, home of the  
161 wolves whose tracking data are used in this study. C) Lobinha (one of the individuals from our  
162 study), a female maned wolf of approximately two years old, wearing a GPS tracking collar.

163

164 The main threat to the species comes from the continuous large scale habitat loss (Noss and  
165 Lima, 2007) which is especially significant in Brazil because of the extensive conversion of the  
166 Cerrado (Brazilian savannah) into farmland (Fonseca *et al.*, 1994). Only 20% of Cerrado is still  
167 covered by native vegetation (Myers *et al.*, 2000) and less than 2.5% is protected by law. One  
168 of the protected areas, the Serra da Canastra National Park (CNP) (Figure 1B) has been key to  
169 the preservation of maned wolves. The extensive conversion of the park's surroundings into  
170 farmland has exposed the wolves to many anthropogenic threats, such as road traffic, culling  
171 and disease contamination by domestic animals (Deem and Emmons, 2005), all of which can  
172 result in large fluctuations in population size, eventually leading to extinction (de Paula and  
173 Desbiez, 2014).

174 Understanding interactions with the environment and relevance of different habitats for survival  
175 is of prime importance for preserving a species (Garshelis, 2000). There has been only one  
176 study based on GPS and satellite data on the habitat use by maned wolves, and it was restricted  
177 to one male and one female (Coelho *et al.*, 2008). Most studies on maned wolves were  
178 performed in a captive population and little is known about maned wolves in the wild (Bueno  
179 and Motta-Junior, 2009; de Paula *et al.*, 2013).

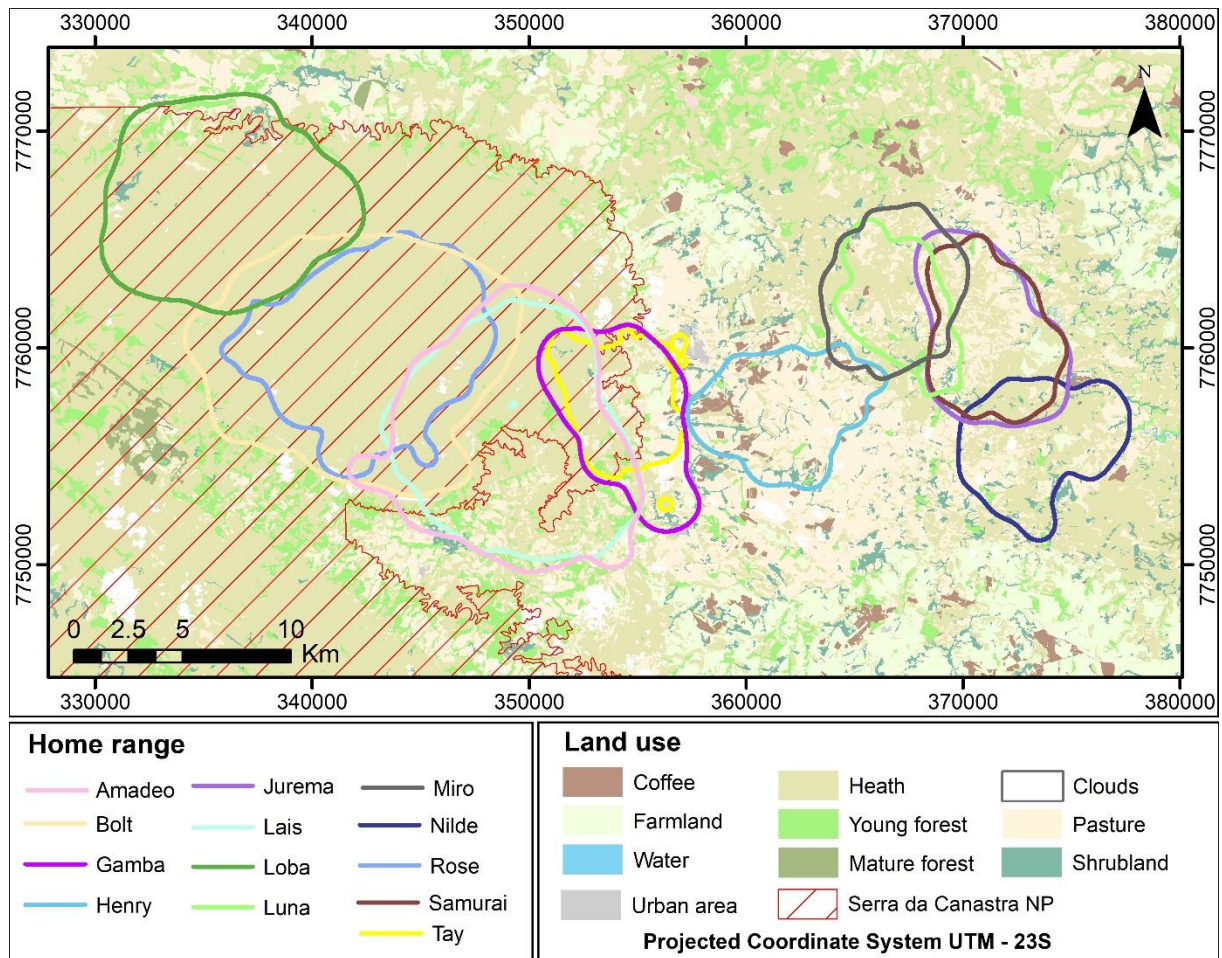
180

## 181 **2.2. GPS tracking data**

182 Tracking data were collected using GPS collars - (Pinnacle Lite G5C 275D by Sirtrac, 3300S  
183 and Iridium Track 1D by Lotek Wireless Inc) for 13 maned wolves between March 2007 and

184 July 2015 (see Table 1 in Supplementary information A for a summary of the tracking data),  
185 the most complete attempt to study this species to date (de Paula, 2016). Our sample included  
186 seven females and six males, with the tracking period varying from 59 to 841 days per  
187 individual. We calculated home ranges of each individual as the 95% isopleth from kernel  
188 density utilisation distribution (UD) surfaces to show the extent of territories (Worton, 1989)  
189 of each individual's GPS tracking data (Figure 3). A home range is defined as a set of bounded  
190 areas used by an animal in the course of its normal activities, such as foraging and mating (Burt,  
191 1943) and is typically calculated as an isopleth of the UD density estimate.

192 Home ranges varied in size with an average of  $64.5 \text{ km}^2 \pm 34.5 \text{ km}^2$  standard deviation but were  
193 generally compact in shape. Only two individuals stay completely within the CNP, five transit  
194 between the CNP and its surrounding areas, and the remaining six are based outside the park in  
195 landscapes extremely influenced by anthropogenic activity (primarily agriculture) (Figure 3).  
196 Maned wolves are known to be territorial, and we found that home ranges had generally little  
197 overlap, except between mates (Figure 3).



198

199 Figure 3 - Home ranges (95% utilization distribution) for each individual and Canastra National  
 200 Park (CNP) limits overlaid on top of land use classes. Home ranges of the two individuals in  
 201 each couple (Table 1 in Supplementary information A) intersect to a large extent. The land use  
 202 map was produced by (de Paula, 2016) based on automatic and supervised multi-temporal  
 203 classification (2009 - 2011) of RapidEye images with 5 m spatial resolution.

### 204 2.3. Remote sensing data

205 We integrate coarse spatial resolution - fine temporal resolution MODIS (Moderate Resolution  
 206 Imaging Spectroradiometer) data and higher spatial resolution - coarse temporal resolution data  
 207 from Terra - ASTER (Advanced Spaceborne Thermal Emission and Reflection Radiometer),  
 208 Landsat 4-5-7-8, CBERS 2 (China-Brazil Earth Resources Satellite) and CBERS 2B) (Table 1)  
 209 to create a high spatial and temporal granularity NDVI data set (Multi-Source Data Fusion

210 product, MF-NDVI). We use data from the same seven higher spatial resolution - coarse  
 211 temporal resolution data sensor to calculate fine spatial resolution - coarse temporal resolution  
 212 NDVI (Multi-Source Data product, MS-NDVI). We also use the daily reflectance (MOD09  
 213 product) to calculate coarse spatial resolution fine temporal resolution NDVI (Single-Source  
 214 Data product, SS-NDVI) and cloud mask (MOD35 product) products to filter out clouds, both  
 215 products from Terra - MODIS. Our study period spans from 2007 to 2013, and during this  
 216 period we acquired 2260 total images, with the vast majority (2227) coming from MODIS (due  
 217 to high temporal resolution) and 33 images coming from the other sensors (Table 1). We only  
 218 retrieved images with cloud coverage lower than 5%.

219 Table 1 - Remote sensing data used as input for the SS, MS and MF approach to produce NDVI  
 220 data sets. The letters along with spatial resolutions are specifying the spectral bands for sensors  
 221 with multiples spatial resolutions, sensors without letters have a uniform spatial resolution  
 222 along the spectral bands. R stands for red, G for green, B for blue, NIR for near infra-red, VNIR  
 223 for visible (RGB) and near infra-red, SWIR for short wavelength infra-red, FI for far infra-red  
 224 and TIR for thermal infra-red.

<i>Satellite</i>	<i>Sensor</i>	<i>Temporal resolution (days)</i>	<i>Spatial resolution (m)</i>	<i>Images used</i>
CBERS 2-2B	High Resolution CCD Camera (HRCC)	26	20	3
Landsat 4-5	Thematic Mapper (TM)	16	30	16
Landsat 7	Enhanced Thematic Mapper plus (ETM+)	16	30	

Landsat 8	Operational Land Imager (OLI)	16	30	14
Terra	Moderate Resolution Imaging Spectroradiometer (MODIS)	1 - 2	250 (R/NIR) 500 (B/G/SWIR) 1000 (VNIR/FI)	2227
Terra	Advanced Spaceborne Thermal Emission and Reflection Radiometer (ASTER)	16	15(VNIR) 30 (SWIR) 90 (TIR)	3

#### 225      **2.4. Step 1: Multi-source data fusion**

226            We performed the absolute calibration of satellite data to guarantee consistency among  
227 the measurements from different satellites. NDVI growth rates were extracted from MODIS  
228 and we performed land cover classification on the finer resolution data, so that we could  
229 compute land cover fractions within each MODIS pixel. The land cover fraction and the daily  
230 NDVI growth rates from MODIS were used to calculate the NDVI growth rate for each land  
231 cover fraction, which was then applied to the finer NDVI data to generate a time series of daily  
232 NDVI with higher level of spatial detail. In this section we provide the details of this  
233 methodology, while figure 2 illustrates the proposed process.

234

**235 2.4.1. Absolute calibration of remote sensing data**

236 Absolute calibration is necessary to convert the digital numbers stored within a remotely sensed  
237 image to spectral reflectance, the physical quantity of the object (Rees, 2001), which is  
238 important for integrating multi-source remotely sensed data. MODIS data (MOD09) have been  
239 pre-processed to spectral reflectance values, therefore we only calibrated the 33 images from  
240 the other seven satellites. This was done using sensor-specific scaling parameters and equations  
241 that are provided in the meta data for each image and user's handbook of each sensor. We further  
242 re-sampled the 33 images, i.e. all except MODIS, to 15 m in order to match the finest spatial  
243 resolution of our data sets. We used the nearest neighbour method to perform the resampling,  
244 which does not create values that were not in the original data (Meneses and Almeida, 2012).  
245 This is important to preserve the relationship between what was measured on the ground by the  
246 satellite and the biophysical variable being analysed.

**247 2.4.2. Calculating SS-NDVI and MS-NDVI**

248 The calibrated spectral reflectance bands were then used to compute the SS-NDVI (Single  
249 Source) time series with 2227 images based on MODIS data and a MS-NDVI (Multi-Source)  
250 time series with 33 images based on data from the other seven satellites. NDVI is a proxy for  
251 the content and state of the live green vegetation and its computation requires information on

252 the spectral reflectance in the red and near infra-red portions of the electromagnetic spectrum  
253 (Rouse *et al.*, 1973):

$$254 \quad NDVI = \frac{NIR_{\rho} - Red_{\rho}}{NIR_{\rho} + Red_{\rho}} \quad (1)$$

255 Here  $NIR_{\rho}$  is the reflectance in near infra-red interval (800 - 1000 nm<sup>1</sup>) and  $Red_{\rho}$  is the  
256 reflectance in the red interval (650 - 700 nm). NDVI values range from -1 to 1. Values smaller  
257 than 0.1 are usually related to bare rocks, sand, or snow; values around 0.2 to 0.5 are related to  
258 sparse vegetation such as shrub, grasslands or senescence crops; values between 0.6 and 1.0  
259 correspond to dense vegetation, such as tropical forests or crops at their peak growth stage  
260 (Rouse *et al.*, 1973; Xue and Su, 2017).

### 261 **2.4.3. Generating time-series of SS-NDVI growth rates**

262 We calculated the daily NDVI time series, which we here call MF-NDVI (Multi-Source Data  
263 Fusion product), by adapting downscaling methods from Rao *et al.* (2015).

264 MODIS data have been previously used for extracting growth rates and understanding  
265 vegetation dynamics (Lu *et al.*, 2015). Their high temporal resolution allows daily monitoring  
266 of changes in vegetation, however, the extraction of accurate NDVI growth rates requires a  
267 rigorous filtering process to de-noise the data series, i.e., to reduce the known interference of  
268 clouds, atmosphere dynamics, variability on the detectors that register reflectance and other

---

<sup>1</sup> Theoretical limit according to Jensen (2006), these limits may vary from satellite to satellite but will stay within this range.

269 factors. A wavelet transform (WT) is particularly efficient in identifying and reducing noise  
270 while preserving useful information in time-series (Lu *et al.*, 2007) and it has been widely used  
271 in the extraction of vegetation patterns via radiometric indices (Sakamoto *et al.*, 2005;  
272 Priyadarshi *et al.*, 2017).

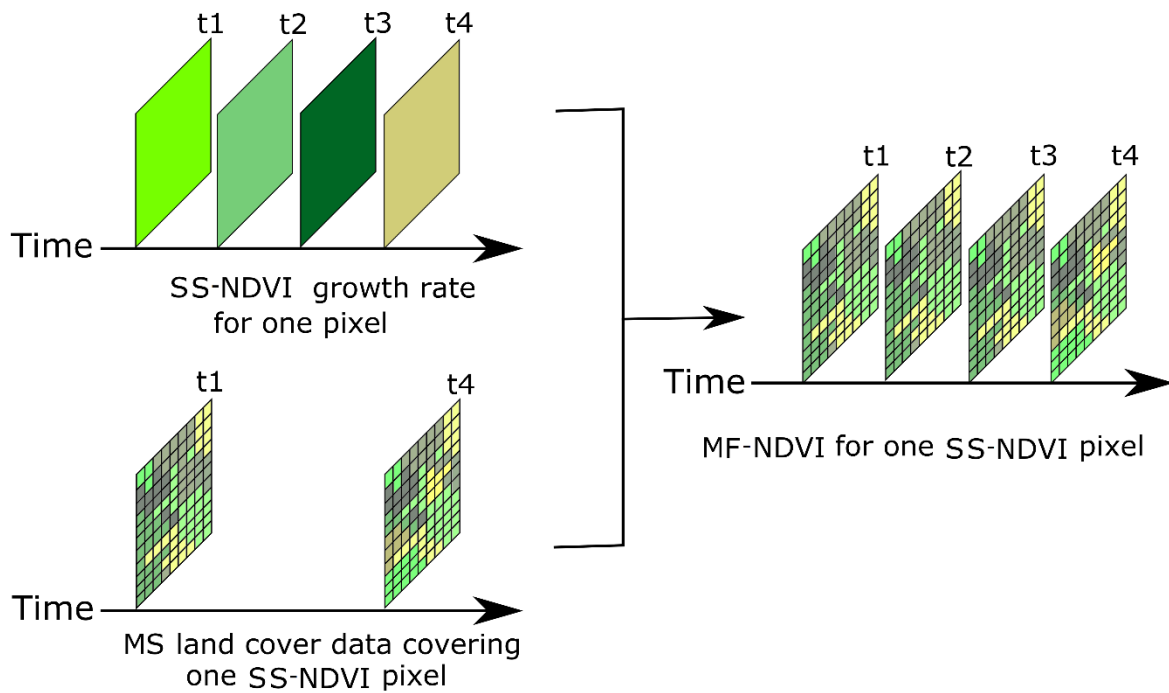
273 We used the 2227 SS-NDVI (Single Source NDVI) images to create a temporal profile of NDVI  
274 for each 250 m pixel in our study area. We first used the cloud mask product (MOD35)  
275 (Strabala, 2018) corresponding to each SS-NDVI image to remove cloud contamination. In the  
276 next step, we converted the images into 46,710 time-series of NDVI values, one time-series for  
277 each 250m pixel, and applied two consecutive WT using the Daubechies 4 mother wavelet  
278 (MW) (Daubechies, 1990). This MW has been extensively used for de-noising and it is  
279 commonly used for NDVI data (Kaddar *et al.*, 2017). We performed a four level soft threshold  
280 WT of the NDVI temporal series for each pixel (2227 samples/pixel) in the MODIS data, then  
281 we reconstructed the series, then repeated the procedure once again to obtain the final filtered  
282 NDVI pixel series. The NDVI daily growth rates were then computed for each pair of SS-NDVI  
283 images by calculating the first derivative for each filtered SS-NDVI pixel time series.

#### 284 **2.4.4. Calculating MF-NDVI**

285 The filtered NDVI daily growth rates extracted from SS-NDVI (Single Source NDVI) reflect  
286 the average of the vegetation dynamics covered by each 250 m x 250 m pixel. To obtain more  
287 detailed information on the vegetation dynamics within each pixel, we calculated the  
288 contribution of each land cover fraction to the growth rates (Rao *et al.*, 2015) (Figure 5).



289



290

291 Figure 4 - The filtered SS-NDVI growth rates are combined with MS land cover data to produce  
 292 the MF-NDVI, which has the same temporal resolution as the SS-NDVI and similar spatial  
 293 details to the MS-NDVI. Land cover data are used to find the NDVI growth rate for each MS  
 294 pixel (15 m). Growth rates are then applied to the available 33 MS-NDVI images to create the  
 295 temporal series of MF-NDVI.

296 To calculate land cover fractions within each SS pixel, the calibrated spectral reflectance bands  
 297 in the finer resolution images were used to obtain 33 land cover maps. We use the BIRCH  
 298 (Balanced Iterative Reducing and Clustering using Hierarchies) algorithm (Zhang,  
 299 Ramakrishnan and Livny, 1996) to perform automatic non-supervised classification. The  
 300 algorithm requires three input parameters: 1) a threshold for the maximum allowed radius for  
 301 the cluster resulting from the grouping of a sub-cluster and the closest sample (the cluster is

302 partitioned if the radius is bigger than the chosen threshold); 2) a branching factor that  
303 determines the maximum number of sub-clusters in each node (if a new sample is added such  
304 that the number of sub-clusters exceeds the branching factor the node is split into two); and 3)  
305 the number of clusters after the final clustering step, which prunes the resulting hierarchical  
306 tree. We used a branching factor of 100 for all images, varied the threshold from 0.2 to 0.7 by  
307 0.02 for each image and did not use pruning. For each threshold we computed the Calinski-  
308 Harabaz Index (CHI) (Calinski and Harabasz, 1974) to measure the intra- and inter-cluster  
309 quality of our land cover classes, and for each image we kept the threshold that achieved the  
310 lowest within-cluster dispersion and highest between-cluster dispersion. This produced the  
311 optimal data-driven unsupervised land cover classification for each image.

312 For each of the 33 land cover classifications (15 m) we then calculated the percentage of each  
313 land cover within the corresponding SS pixel (250 m), which produced 33 maps of land cover  
314 fractions for our study period. The use of multiple land cover fractions maps is important to  
315 account for possible land cover changes within a SS pixel during the study period. The  
316 contribution of each land cover fraction and the growth rates were then applied to the 33 MS-  
317 NDVI (Multi-Source Data product) images to generate the MF-NDVI (Multi-Source data  
318 Fusion product) images (Rao *et al.*, 2015). Mathematical details of our procedure are presented  
319 in Supplementary information B. The assessment of the resultant MF-NDVI time series is  
320 presented in Supplementary information C.

## 321 **2.5. Step 2: Context-aware movement analysis**

### 322 **2.5.1. Linking NDVI data sets and wildlife tracking data**

323 To explore which of the three different NDVI data sets better predict wolves' habitat selection,  
324 we annotated the wildlife tracking data with NDVI values from each of the three data sets and  
325 used Step Selection Functions (SSF) to assess NDVI effects on movement probability. We  
326 linked GPS fixes to the NDVI datasets by matching both the temporal and spatial coordinates  
327 using the nearest neighbour method (Dodge *et al.*, 2013; Brum-Bastos, Long and Demšar,  
328 2016). We then created SSFs models for each NDVI data set and compared them through  
329 statistical analysis of results from 10-fold cross-validations.

330 SSFs statistically model the effects of landscape on movement probability by contrasting used  
331 and available resources (Equation 2). SSFs require real steps to characterize used resources  
332 and random steps to characterize available resources. Real steps are the locations registered by  
333 tracking data. Random steps are defined from each tracked location by applying a step length  
334 and turning angle, which are drawn from the distributions of step lengths and turning angles  
335 observed from all tracking data (Thurfjell, Ciuti and Boyce, 2014).

$$336 \quad w(x) = \exp(\beta_1 x_1 + \beta_2 x_2 + \dots + \beta_p x_n) \quad (2)$$

337 where  $w(x)$  is the likelihood of a step (random or real) with the associated resources  $x = x_1$  to  
338  $x_n$  being used by the animal, and  $\beta_1$  to  $\beta_p$  are coefficients estimated by conditional logistic  
339 regression for the associated resources (Fortin *et al.*, 2005). Steps with a higher SSF score  $w(x)$   
340 have a higher likelihood of being chosen by the tracked animal.

341 We created five random steps for each GPS location as recommended by (p.6 Thurfjell, Ciuti  
342 and Boyce, 2014), which were defined by randomly drawing a step length and a turning angle  
343 from the observed distributions of these parameters. Similarly, to the GPS points, random steps  
344 were also annotated with NDVI values from the three NDVI data sets. Next, we perform a 10-  
345 fold cross-validation by training the SSF model on one-fold (GPS points and random steps) and  
346 predicting only on the GPS points (used resources) of the remaining folds. As Steps with a  
347 higher SSF score  $w(x)$  have a higher likelihood of being chosen by the tracked animal, we can  
348 use the prediction on used areas (GPS points only) to compare which NDVI data set is more  
349 accurate in predicting habitat use. We do this by calculating and comparing the sum of the  
350 logged odds for each fold cross-validation for the three NDVI datasets. As a used resource or  
351 GPS point should have  $w(x) = 1$  and  $\log(1) = 0$ , the best model is the one that yields the  
352 maximum of the summed log-odds. We use ANOVA and Students T-tests to assess differences  
353 between the three data sets. We also retrieve and compare the distribution of angular  
354 coefficients and p-values for the three SSF models.

### 355 **3. Results**

#### 356 **3.1. Step 1: Multi-source data fusion**

357 The MS (Multi-Source) approach with higher spatial resolution data was able to provide more  
358 NDVI images than a single-source approach would at the same spatial resolution. However,  
359 even using multiple satellites the NDVI data retrieved covered only 1% of the wildlife tracking  
360 period (Table 2) and there were data gaps as long as almost two years (Figure 4A) due to cloud

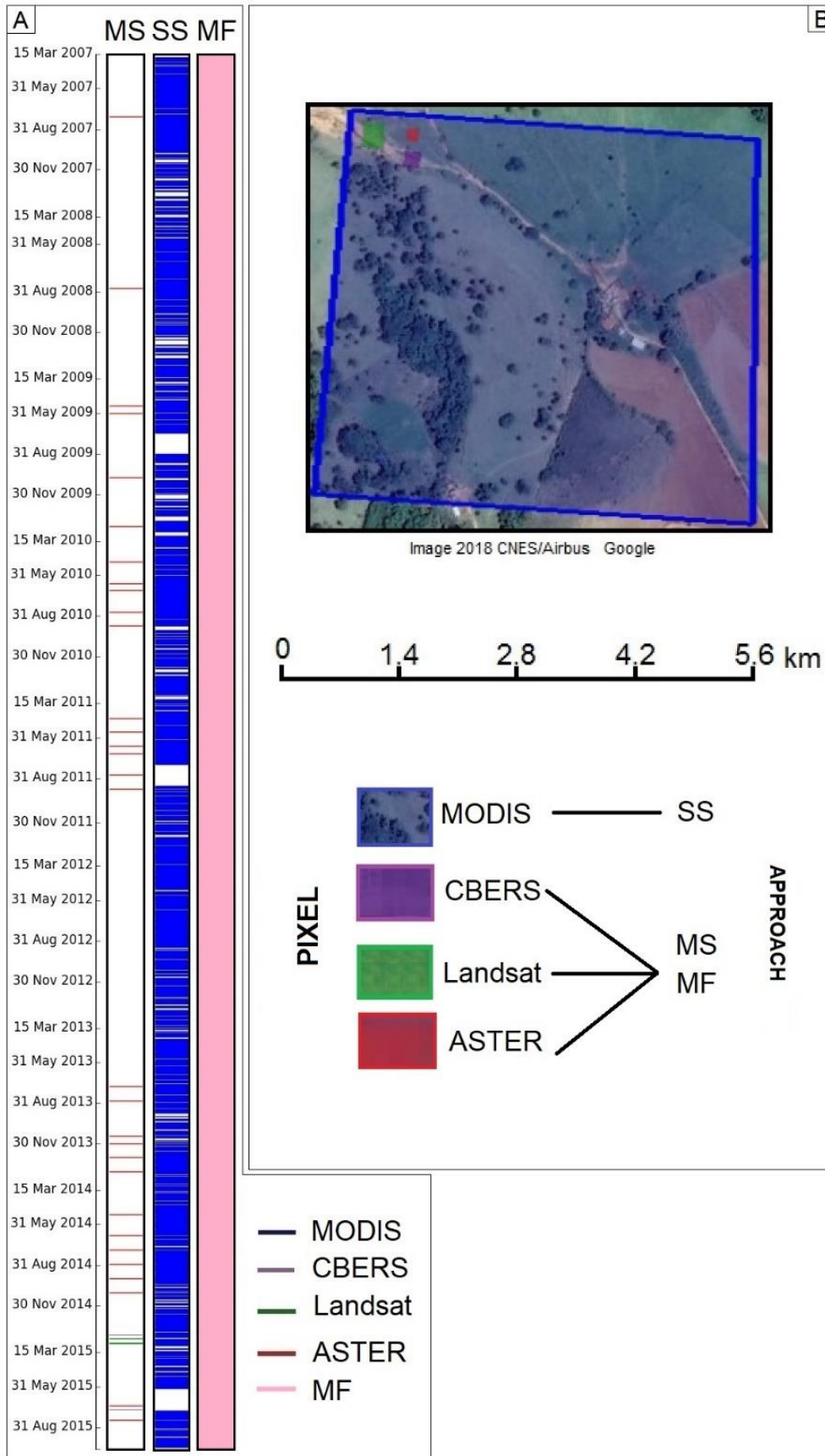
361 coverage. The SS (Single Source) approach with coarse spatial resolution data, which is the  
 362 common practice in movement ecology, was able to provide daily images for 80% of the  
 363 wildlife tracking period (Table 2) with some gaps of approximately two months around August  
 364 (Figure 4A) due to cloud coverage. Finally, the MF (Multi-Source Fusion) provided daily  
 365 images for 100% of the wildlife tracking period (Table 2) (Figure 4A) due to cloud coverage.  
 366 Figure 4B shows scaled pixel sizes overlaying an image from a portion of the study area,  
 367 highlighting how the heterogeneity of environmental conditions might be camouflaged by the  
 368 spatial resolution of the SS approach, but can be captured by the MS and MF approaches.

369 Table 2 - Characteristics of the NDVI data sets produced by the SS, MS and MF approaches.

<i>Approach</i>	<i>Number of NDVI images</i>	<i>Tracking days covered (%)</i>	<i>Revisiting time (days)</i>	<i>Spatial detail (m)</i>
<i>SS</i>	2227	70	1	250
<i>MS</i>	33	1	< 15*	15-30
<i>MF</i>	3150	100	1	15-30

\*If gaps due to cloud coverage are not considered

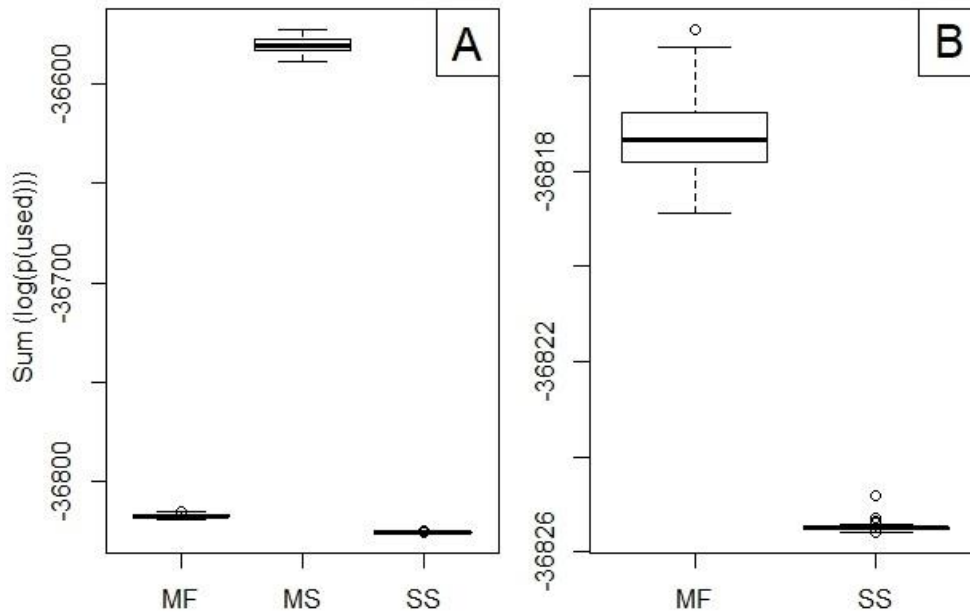
370



372 Figure 5 - Results from the three approaches used to obtain NDVI data sets. Panel A) shows a  
373 timeline covering the wildlife tracking period, where horizontal dashes indicate availability of  
374 NDVI images from each approach. The image source is specified by the colour of the bar shown  
375 in the legend. MF images are plotted on the right timeline, SS images are plotted in the middle  
376 timeline and MS images are plotted on the left timeline. Panel B) shows scaled pixel sizes  
377 overlaying an image from a portion of the study area, highlighting how the heterogeneity of  
378 environmental conditions might be camouflaged by the spatial detail level of the SS approach.  
379 A SS pixel covers 62500 m<sup>2</sup> and originally the data used to produce MS and MF images were  
380 as follows: a Landsat pixel covers 900 m<sup>2</sup>, a CBERS pixel covers 400 m<sup>2</sup> and an ASTER pixel  
381 covers 225 m<sup>2</sup>. However, they were all re-sampled to 15 m pixel size covering 225 m<sup>2</sup>.

### 382 **3.2. Step 2: Context-aware movement analysis**

383 We found that the MS-NDVI (Multi-Source NDVI) had the highest predictive probability  
384 (largest log-odds) based on our k-fold cross validation procedure. This was followed by the  
385 MF-NDVI (Multi-Source Fusion) and lastly the SS-NDVI (Single Source) data (Figure 6A).  
386 Therefore, the model that included only the high spatial resolution satellites (but not the high  
387 temporal resolution MODIS NDVI data) was the best at predicting habitat selection in terms of  
388 NDVI. The poorest performing model was the SS-NDVI model. The MF model therefore  
389 achieved a relatively middle performance level, falling in between the MS-NDVI and the SS-  
390 NDVI (Figure 6B).



391

392 Figure 6 - Sum of logged predicted probabilities for used areas (GPS points) for each of the ten-

393 fold cross validations performed for each step-selection model. Panel A shows the results for

394 MF-, MS- and SS-NDVI. Panel B zooms in to the results of MF and SS-NDVI.

395 The ANOVA indicates that the use of different NDVI data sets have a statistically significant

396 effect ( $p\text{-value} < 0.01$ ) on the sum of the logged predicted probabilities for the GPS points

397 (used areas). Pairwise Students T-tests indicated that the MS-NDVI produced superior models

398 in comparison to the other two data sets ( $p\text{-value} < 0.01$ ) and that the MF-NDVI performed399 significantly better than SS-NDVI ( $p\text{-value} < 0.01$ ).

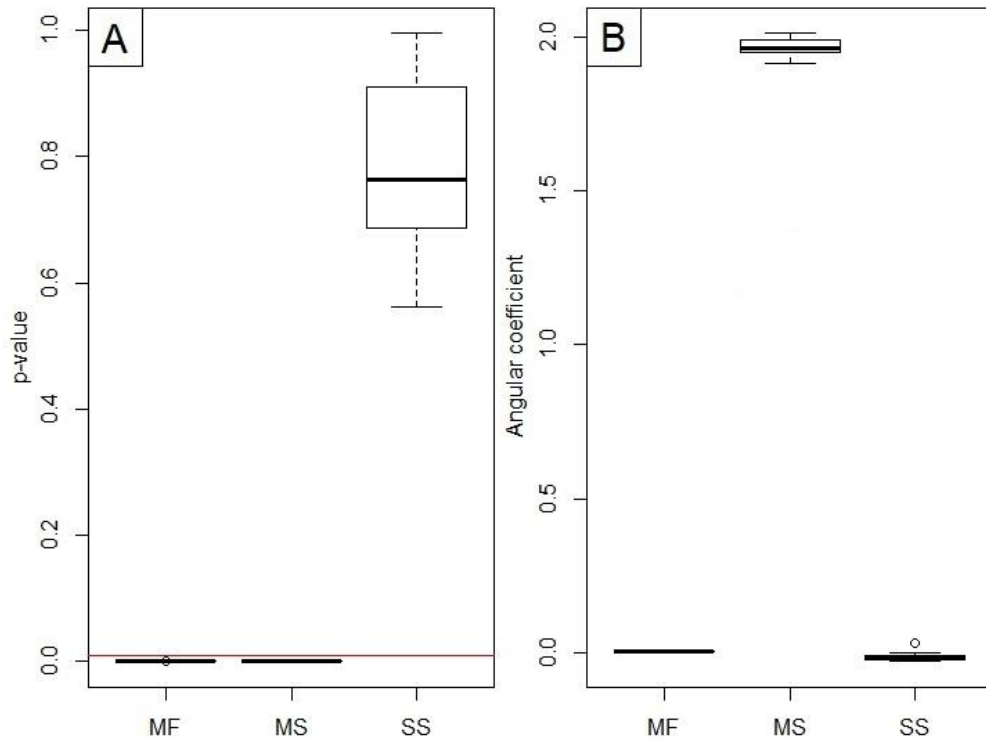
400 Importantly, the NDVI coefficient was not significant in the SS-NDVI SSF models but was

401 always significant in the models using MS-NDVI and MF-NDVI (Figure 7). The coefficients

402 for NDVI ranged between 1.9 and 2.0 in the MS-NDVI model and were always under 0.02 in

403 the other two models MF- and SS-NDVI.





404

405 Fig 7 - Distribution of the parameters from the ten Step-Selection Functions generated for with  
 406 each NDVI data set. Panel A shows the p-values for MF-, MS- and SS-NDVI; the red line  
 407 indicates p-value = 0.01. Panel B shows the SSF angular coefficients for NDVI for MF-, MS-  
 408 and SS-NDVI.

#### 409 4. Discussion and conclusion

410 In this paper, we used multi-source data fusion to combine MODIS data with higher spatial  
 411 resolution data (ASTER, Landsat 4-5-7-8, CBERS 2-2B) and created a synthetic NDVI product  
 412 with a 15 m spatial detail and daily temporal resolution (MF-NDVI). We also used the higher  
 413 spatial resolution data to create a multi-source NDVI product (MS-NDVI) with same level of  
 414 spatial detail but coarser temporal resolution and data from MODIS to create a single-source  
 415 NDVI product with high temporal resolution but coarse spatial resolution (SS-NDVI). We

416 combined the three different spatial-temporal resolution NDVI products with GPS tracking data  
417 of maned wolves to create step-selection functions (SSF), which are models used in ecology to  
418 investigate and predict habitat selection by animals. We used SSFs to investigate which data  
419 approach created a NDVI dataset with higher accuracy in predicting habitat selection for maned  
420 wolves. In the following we discuss some of advantages and limitations of this approach and  
421 contextualise our findings.

422 We hypothesized that the MF-NDVI data would be best at predicting habitat selection (defined  
423 by NDVI) because these data capture both the fine spatial heterogeneity and temporal dynamics  
424 of primary productivity. However, we found that the MS-NDVI model was the strongest  
425 predictor of habitat selection by maned wolves, and that the SS-NDVI was the poorest predictor.  
426 Therefore, it is perhaps unsurprising that the performance of the MF-NDVI model lied in  
427 between the other two models. This seems to suggest in the case of maned-wolves in the  
428 Brazilian savannah that spatial heterogeneity in the availability of primary productivity is far  
429 more important than the temporal dynamics when predicting fine-scale movement and habitat  
430 selection.

431 MODIS data, which were used in the SS approach, were designed for mapping vegetation at  
432 global, continental or national scale, while the data used for the MS and MF approaches were  
433 designed for mapping vegetation at the community and species level (Xie, Sha and Yu, 2008),  
434 which is closer to the scale at which maned wolves were experiencing the landscape. In animal  
435 ecology, detailed information on habitat allows the representation of the cognitive map of

436 animal's environment and the observation at approximately same spatio-temporal scale as an  
437 observer's experience (Cagnacci *et al.*, 2010), which is important for understanding individual's  
438 decision making processes. In addition, the MF approach had performance in between the SS  
439 and the MS, which makes sense as this product is a combination of the two previous ones and  
440 some of the interval we have between the MS scenes are probably too long to allow changes on  
441 vegetation be modelled as a linear function, which added uncertainty to the MF-NDVI. In  
442 addition, the MF approach requires a sufficient number of landcover classifications adequately  
443 distributed across the study period. Ideally, there would be one landcover classification for each  
444 15 days interval, but that can be especially difficult to guarantee in areas with high cloud  
445 coverage, such as the Amazon forest, or during specific seasons, such as the wet season in the  
446 Atlantic forest. Moreover, this approach has higher data and computational complexity, which  
447 can be challenging for researchers that are no acquainted with advanced remote sensing  
448 techniques. Lastly, it is difficult to obtain ground truth data to validate the product generated  
449 by the MF approach, as it ideally it would require either fieldwork sampling on different days,  
450 or leaving out MS images and trying to reproduce them with the MF approach for comparison.  
451 The validation itself can take as much or more time than processing the data, but it is necessary  
452 to know if the data will actually be representing the experience of an individual in that  
453 landscape. Still, the MF approach performed better than what is traditionally used in movement  
454 ecology

455 The temporal resolution of data produced using a multi-sensor approach might drastically  
456 improve in areas less densely covered by clouds. We had bigger relatively large data gaps in  
457 our MS-NDVI data because we were extremely conservative with the cloud coverage threshold  
458 for accepting images ( $< 5\%$ ), particularly for an area that is known to have a concentrated and  
459 seasonal rainfall regime. Another reason for our conservative threshold was the use of these  
460 images for creating the MS-NDVI data set, which requires scenes with clear sky.

461 In terms of new insights into movement behaviour, the SSF model of each NDVI data set  
462 reported different relationships between vegetation and maned wolves' movement. The  
463 traditional SS approach reported no statistically significant relationship between vegetation and  
464 habitat selection for maned wolves, whilst the MS and MF models, which had higher spatial  
465 resolution, reported a statistically significant relationship. This differences in significance of  
466 vegetation for habitat selection reinforce the capacity of multi-source and multi-source data  
467 fusion methods to provide new insights into movement analysis when compared to the  
468 traditional single-source approaches. In addition, the difference between the distributions of the  
469 NDVI coefficients for each model highlights once again that much of the patterns we see are  
470 related to the granularity and scale of the data we use (Laube and Purves, 2011). Therefore,  
471 when selecting earth observation data for movement analysis, it is essential to consider the  
472 scales of the movement but also the scales of the earth observation data being linked to  
473 movement. The goal is to capture data that can portray the changes in environmental conditions  
474 that closely match the reality perceived by the individual moving, i.e., at the spatial and

475 temporal scale at which the individual is interacting with environment. Multi-source and multi-  
476 source data fusion methodologies offer tremendous potential in the study of wildlife movement,  
477 because these data will better match the spatial heterogeneity and temporal dynamics associated  
478 with environmental conditions experienced by wildlife.

479 The three approaches we tested (i.e., using single source data, combining multiple medium/high  
480 resolution sensor data and fusing these data with high temporal resolution Earth observation  
481 data) are not limited to optical satellite imagery, but can be used for other types of Earth  
482 observation data captured using a variety of other sensors. For example, different satellite  
483 systems are now collecting detailed information on environmental conditions such as, water  
484 content, chlorophyll, snow coverage, vegetation type, land or sea surface temperature,  
485 humidity, rainfall, air pressure and Earth's magnetic field (Sadeghi *et al.*, 2018), which can be  
486 useful for explaining wildlife movement patterns. There is a potential to extend our  
487 methodology beyond optical imagery and include all these different types of environmental  
488 data. We note here that we found that a multi-source approach was more predictive of  
489 movement and habitat selection than a multi-source fusion approach, and we recommend that  
490 future research first explores the use of multi-source Earth observation data for movement  
491 analysis at local and spatially detailed scales. Further, a multi-source approach is less  
492 computationally demanding than multi-source data fusion methods, which may not lead to  
493 improvements in predictive capability as shown here. Moreover, the need to ensure enough  
494 landcover classifications at reasonable intervals it is important to highlight that

495 This paper is, as far as we are aware, one of the first attempts to combine data from multiple  
496 satellites and sensors for the purpose of analysing animal movement patterns (but see Berman  
497 *et al.*, 2019) . While remotely sensed data has become more widely used in movement ecology  
498 studies, using data from more than one source (either in a multi-source or a multi-source data  
499 fusion context) and linking these data to yet another complex data source (i.e., GPS tracking  
500 data) is a complicated task (as demonstrated by the procedures used in this paper) that many  
501 ecologists may still refrain from undertaking (Pettorelli *et al.*, 2014). The primary conceptual  
502 challenge in this process is the mismatch between the spatial and temporal resolutions of  
503 different sources of satellite remotely sensed data and wildlife tracking data – in this paper we  
504 demonstrated how this challenge can be tackled by applying multi-source and multi-source data  
505 fusion techniques.

506 Monitoring changes in the biosphere across sufficient spatial and temporal scales and linking  
507 the information on these changes with detailed *in situ* data, such as wildlife tracking data,  
508 represents an area of opportunity for further discovery in the field of movement ecology. While  
509 there are a number of tools that can support this process, methods for combining remote sensing  
510 data with wildlife tracking data are still in their infancy (Neumann *et al.*, 2015; Remelgado,  
511 Wegmann and Safi, 2019). As demonstrated here, these analyses can be undertaken using  
512 relatively simple single-source remotely sensed data but become increasingly complex as  
513 multiple sources of earth observation data are included, and further complicated when using  
514 true data fusion methods. Here we find that (in the case of a terrestrial omnivore) a multi-source

515 approach that focuses on high spatial resolution data, outperforms single source high temporal  
516 resolution data, and a more complex multi-source fused dataset. Thus, future research may wish  
517 to first explore multi-source high resolution datasets where the spatial heterogeneity of  
518 resources is more likely to be predictive of movement and habitat selection over temporal  
519 dynamics. In contrast, in species where temporal dynamics are crucial to movement and habitat  
520 selection, high temporal resolution earth observation data or a more multi-source data fusion  
521 approach (as demonstrated here) are likely to provide higher predictive outcomes, leading to  
522 better insights in to the movement of wildlife species.

523 **Funding:** This work was supported by CAPES (Coordination for the Improvement of Higher  
524 Education Personnel) [BEX-13438-13-1].

## 525 **Acknowledgments**

526 The authors would like to acknowledge Dr Dylan Connor at Arizona State University for his  
527 help with statistical concepts.

## 528 **References**

- 529 Bartlam-Brooks, H. L. A. *et al.* (2013) ‘In search of greener pastures: Using satellite images  
530 to predict the effects of environmental change on zebra migration’, *Journal of Geophysical*  
531 *Research: Biogeosciences*. Wiley-Blackwell, 118(4), pp. 1427–1437. doi:  
532 10.1002/jgrg.20096.
- 533 Berman, E. E. *et al.* (2019) ‘Grizzly bear response to fine spatial and temporal scale spring  
534 snow cover in Western Alberta’, *PLoS ONE*, 14(4). doi: 10.1371/journal.pone.0215243.
- 535 Brum-Bastos, V., Long, J. and Demšar, U. (2016) ‘Dynamic trajectory annotation for  
536 integrating environmental and movement data’, in *Visually-supported Computational*  
537 *Movement Analysis Workshop - AGILE 2016*. Helsinki. Available at:  
538 [http://viz.icaci.org/vcma2016/wp-content/uploads/2016/07/vcma\\_brumbastos-paper.pdf](http://viz.icaci.org/vcma2016/wp-content/uploads/2016/07/vcma_brumbastos-paper.pdf).
- 539 Brum-Bastos, V. S., Long, J. A. and Demšar, U. (2018) ‘Weather effects on human mobility:

- 540 a study using multi-channel sequence analysis’, *Computers, Environment and Urban Systems*.  
541 Pergamon, 71, pp. 131–152. doi: 10.1016/J.COMPENVURBSYS.2018.05.004.
- 542 Buchin, K. *et al.* (2015) ‘Deriving movement properties and the effect of the environment  
543 from the Brownian bridge movement model in monkeys and birds’, *Movement Ecology*.  
544 BioMed Central, 3(1), p. 18. doi: 10.1186/s40462-015-0043-8.
- 545 Bueno, A. de A. and Motta-Junior, J. C. (2009) ‘Feeding habits of the maned wolf,  
546 *Chrysocyon brachyurus* (Carnivora: Canidae), in southeast Brazil’, *Studies on Neotropical*  
547 *Fauna and Environment*. Taylor & Francis, 44(2), pp. 67–75. doi:  
548 10.1080/01650520902891413.
- 549 Böhne, H. and Petteorelli, N. (2017) ‘Better together: Integrating and fusing multispectral and  
550 radar satellite imagery to inform biodiversity monitoring, ecological research and  
551 conservation science’, *Methods in Ecology and Evolution*, 38(1), pp. 42–49. doi:  
552 10.1111/2041-210X.12942.
- 553 Burt, W. H. (1943) ‘Territoriality and Home Range Concepts as Applied to Mammals’,  
554 *Journal of Mammalogy*. Oxford University Press, 24(3), p. 346. doi: 10.2307/1374834.
- 555 Cagnacci, F. *et al.* (2010) ‘Animal ecology meets GPS-based radiotelemetry: a perfect storm  
556 of opportunities and challenges.’, *Philosophical transactions of the Royal Society of London.*  
557 *Series B, Biological sciences*, 365(1550), pp. 2157–62. doi: 10.1098/rstb.2010.0107.
- 558 Calinski, T. and Harabasz, J. (1974) ‘A dendrite method for cluster analysis’,  
559 *Communications in Statistics - Theory and Methods*, 3(1), pp. 1–27. doi:  
560 10.1080/03610927408827101.
- 561 Coelho, C. M. *et al.* (2008) ‘Habitat Use by Wild Maned Wolves ( *Chrysocyon brachyurus* )  
562 in a Transition Zone Environment’, *Journal of Mammalogy*. Oxford University Press (OUP),  
563 89(1), pp. 97–104. doi: 10.1644/06-mamm-a-383.1.
- 564 Daubechies, I. (1990) ‘The wavelet transform, time-frequency localization and signal  
565 analysis’, *IEEE Transactions on Information Theory*, 36(5), pp. 961–1005. doi:  
566 10.1109/18.57199.
- 567 Deem, S. L. and Emmons, L. H. (2005) ‘Exposure of free-ranging maned wolves  
568 (*Chrysocyon brachyurus*) to infectious and parasitic disease agents in the Noël Kempff  
569 Mercado national park, Bolivia’, *Journal of Zoo and Wildlife Medicine*, 36(2), pp. 192–197.  
570 doi: 10.1638/04-076.1.
- 571 Demšar, U. *et al.* (2015) ‘Analysis and visualisation of movement: an interdisciplinary  
572 review’, *Movement Ecology*. BioMed Central, 3(1), p. 5. doi: 10.1186/s40462-015-0032-y.
- 573 Dodge, S. *et al.* (2013) ‘The environmental-data automated track annotation (Env-DATA)  
574 system: linking animal tracks with environmental data’, *Movement Ecology*, 1(1), p. 3. doi:  
575 10.1186/2051-3933-1-3.
- 576 Fonseca, G. A. B. *et al.* (eds) (1994) *Livro vermelho dos mamíferos ameaçados de extinção*.  
577 1st edn. Belo Horizonte, Brazil: Fundação Biodiversitas.
- 578 Fortin, D. *et al.* (2005) ‘Wolves Influence Elk Movements: Behavior Shapes a Trophic  
579 Cascade in Yellowstone National Park’, *Ecology*, 86(5), pp. 1320–1330. doi: 10.1890/04-  
580 0953.
- 581 Fryxell, J. M. *et al.* (2008) ‘Multiple movement modes by large herbivores at multiple



- 582 spatiotemporal scales', *Proceedings of the National Academy of Sciences*. National Academy  
583 of Sciences, 105(49), pp. 19114–19119. doi: 10.1073/pnas.0801737105.
- 584 Garshelis, D. L. (2000) 'Delusions in habitat evaluation: measuring use, selection, and  
585 importance.', in Boitani, L. and Fuller, T. K. (eds) *Research techniques in animal ecology:  
586 controversies and consequences*. New York: Columbia University Press.
- 587 Henry, D. A. W., Ament, J. M. and Cumming, G. S. (2015) 'Exploring the environmental  
588 drivers of waterfowl movement in arid landscapes using first-passage time analysis',  
589 *Movement Ecology*. BioMed Central, 4(1), p. 8. doi: 10.1186/s40462-016-0073-x.
- 590 Howey, L. A. *et al.* (2017) 'Biogeophysical and physiological processes drive movement  
591 patterns in a marine predator', *Movement Ecology*. BioMed Central, 5(1), p. 16. doi:  
592 10.1186/s40462-017-0107-z.
- 593 ICMBio (2016) *Executive Summary Brazil Red Book of Threatened Species of Fauna*.  
594 Available at: [www.icmbio.gov.br](http://www.icmbio.gov.br) (Accessed: 16 September 2018).
- 595 Jensen, J. R. (2006) 'Active and Passive Microwave Remote Sensing', in Clarck, K. C. (ed.)  
596 *Remote Sensing of the Environment: An Earth Resource Perspective*. 2<sup>a</sup>. Englewood Cliffs:  
597 Prentice Hall, p. 592.
- 598 Kaddar, B. *et al.* (2017) 'Spatiotemporal Analysis for NDVI Time Series Using Local Binary  
599 Pattern and Daubechies Wavelet Transform', *International Review of Aerospace Engineering*  
600 (*IREASE*). Praise Worthy Prize, 10(2), p. 96. doi: 10.15866/irease.v10i2.11873.
- 601 Kappes, M. A. *et al.* (2015) 'Reproductive constraints influence habitat accessibility,  
602 segregation, and preference of sympatric albatross species', *Movement Ecology*, 3(1), p. 34.  
603 doi: 10.1186/s40462-015-0063-4.
- 604 Kerr, J. T. and Ostrovsky, M. (2003) 'From space to species: ecological applications for  
605 remote sensing', *Trends in Ecology & Evolution*. Elsevier Current Trends, 18(6), pp. 299–  
606 305. doi: 10.1016/S0169-5347(03)00071-5.
- 607 Laube, P. and Purves, R. S. (2011) 'How fast is a cow? Cross-Scale Analysis of Movement  
608 Data', *Transactions in GIS*. Wiley/Blackwell (10.1111), 15(3), pp. 401–418. doi:  
609 10.1111/j.1467-9671.2011.01256.x.
- 610 Lu, L. *et al.* (2015) 'Evaluation of Three MODIS-Derived Vegetation Index Time Series for  
611 Dryland Vegetation Dynamics Monitoring', *Remote Sensing*, 7(6), pp. 7597–7614. doi:  
612 10.3390/rs70607597.
- 613 Lu, X. *et al.* (2007) 'Removal of Noise by Wavelet Method to Generate High Quality  
614 Temporal Data of Terrestrial MODIS Products', *Photogrammetric Engineering & Remote  
615 Sensing*, 73(10), pp. 1129–1139. doi: 10.14358/PERS.73.10.1129.
- 616 Meneses, P. R. and Almeida, T. De (2012) *Processamento digital de imagens*. Edited by  
617 UNB. Brasília.
- 618 Van Moorter, B. *et al.* (2009) 'Memory keeps you at home: a mechanistic model for home  
619 range emergence', *Oikos*, 118(5), pp. 641–652. doi: 10.1111/j.1600-0706.2008.17003.x.
- 620 Morales, J. M. and Ellner, S. P. (2002) 'Scaling up animal movements in heterogeneous  
621 landscapes: the importance of behavior', *Ecology*, 83(8), pp. 2240–2247. doi: 10.1007/978-  
622 94-017-9523-4\_10.
- 623 Morelle, K. *et al.* (2017) 'From animal tracks to fine-scale movement modes: a

- 624 straightforward approach for identifying multiple spatial movement patterns’, *Methods in*  
625 *Ecology and Evolution*, 8(11), pp. 1488–1498. doi: 10.1111/2041-210X.12787.
- 626 Myers, N. *et al.* (2000) ‘Biodiversity hotspots for conservation priorities’, *Nature*. Nature  
627 Publishing Group, 403(6772), pp. 853–858. doi: 10.1038/35002501.
- 628 Nathan, R. *et al.* (2008) ‘A movement ecology paradigm for unifying organismal movement  
629 research’, *Proceedings of the National Academy of Sciences*, 1035(49), pp. 19052–19059. doi:  
630 101073.
- 631 Neumann, W. *et al.* (2015) ‘Opportunities for the application of advanced remotely-sensed  
632 data in ecological studies of terrestrial animal movement’, *Movement Ecology*, 3(1), p. 8. doi:  
633 10.1186/s40462-015-0036-7.
- 634 Noss, A. and Lima, E. D. S. (2007) ‘Vertebrate Conservation and Biodiversity’, (October  
635 2014). doi: 10.1007/978-1-4020-6320-6.
- 636 de Paula, R. C. (2016) *Adequabilidade ambiental dos biomas brasileiros à ocorrência do*  
637 *lobo-guará (Chrysocyon brachyurus) e efeitos da composição da paisagem em sua ecologia*  
638 *espacial, atividade e movimentação*. University of São Paulo. Available at:  
639 <http://www.teses.usp.br/teses/disponiveis/11/11150/tde-05072016-114911/pt-br.php>.
- 640 de Paula, R. C. and DeMatteo, K. (2015) ‘Chrysocyon brachyurus, Maned Wolf’, in *The*  
641 *IUCN Red List of Threatened Species*. doi: 10.2305/IUCN.UK.2015.
- 642 de Paula, R. C. and Desbiez, A. L. . (2014) ‘Maned wolf population viability’, in Consorte-  
643 McCrea, A. G. and Santos, E. . (eds) *Ecology and conservation of Manned Wolf:*  
644 *Multidisciplinary perspectives*. 1st edn. Boca Raton, FL, p. 322.
- 645 de Paula, R. *et al.* (2013) ‘The Maned Wolf Conservation Project’, in *Ecology and*  
646 *Conservation of the Maned Wolf*. CRC Press, pp. 177–192. doi: 10.1201/b15607-17.
- 647 Pettorelli, N. *et al.* (2006) ‘Using a proxy of plant productivity (NDVI) to find key periods for  
648 animal performance: The case of roe deer’, *Oikos*. Wiley/Blackwell (10.1111), 112(3), pp.  
649 565–572. doi: 10.1111/j.0030-1299.2006.14447.x.
- 650 Pettorelli, N. *et al.* (2011) ‘The Normalized Difference Vegetation Index (NDVI): Unforeseen  
651 successes in animal ecology’, *Climate Research*, 46(1), pp. 15–27. doi: 10.3354/cr00936.
- 652 Pettorelli, N. *et al.* (2014) ‘Satellite remote sensing for applied ecologists: opportunities and  
653 challenges’, *Journal of Applied Ecology*. Edited by E. J. Milner-Gulland. John Wiley & Sons,  
654 Ltd (10.1111), 51(4), pp. 839–848. doi: 10.1111/1365-2664.12261.
- 655 Priyadarshi, N. *et al.* (2017) ‘Reconstruction of time series MODIS EVI data using de-noising  
656 algorithms’, *Geocarto International*, pp. 1–19. doi: 10.1080/10106049.2017.1333535.
- 657 Rao, Y. *et al.* (2015) ‘An Improved Method for Producing High Spatial-Resolution NDVI  
658 Time Series Datasets with Multi-Temporal MODIS NDVI Data and Landsat TM/ETM+  
659 Images’, *Remote Sensing*. Multidisciplinary Digital Publishing Institute, 7(6), pp. 7865–7891.  
660 doi: 10.3390/rs70607865.
- 661 Rees, W. G. (2001) *Physical Principles of Remote Sensing*. 2<sup>a</sup>. Cambridge: Cambrydge  
662 University Press.
- 663 Remelgado, R., Wegmann, M. and Safi, K. (2019) ‘RSMOVE and R package to bridge  
664 remote sensing and movement ecology’, *Methods in Ecology and Evolution*. Edited by L.  
665 Börger. British Ecological Society, 10(8), pp. 1212–1221. doi: 10.1111/2041-210X.13199.

- 666 Rouse, J. W. *et al.* (1973) ‘Monitoring vegetation systems in the Great Plains with ERTS’, in  
667 Freden, S. C. and Becker, M. A. (eds) *Third ERTS Symposium*. Greenbelt: National Library of  
668 Agriculture (NAL) (SP-351, 3010-317), pp. 309–317.
- 669 Sadeghi, M. *et al.* (2018) ‘Remote Sensing of Environmental Variables and Fluxes’, in  
670 *Handbook of Environmental Engineering*. Hoboken, NJ, USA: John Wiley & Sons, Inc., pp.  
671 249–302. doi: 10.1002/9781119304418.ch9.
- 672 Sakamoto, T. *et al.* (2005) ‘A crop phenology detection method using time-series MODIS  
673 data’, *Remote Sensing of Environment*. Elsevier, 96(3–4), pp. 366–374. doi:  
674 10.1016/j.rse.2005.03.008.
- 675 Schneider, D. C. (2001) ‘The rise of the concept of scale in ecology’, *BioScience*, 51(7), pp.  
676 545–554.
- 677 Strabala, K. (2018) ‘MODIS Cloud Mask User’s Guide’, p. 32. Available at:  
678 <http://cimss.ssec.wisc.edu/modis/CMUSERSGUIDE.PDF> (Accessed: 27 June 2018).
- 679 Thorup, K. *et al.* (2017) ‘Resource tracking within and across continents in long-distance bird  
680 migrants’, *Science Advances*. American Association for the Advancement of Science, 3(1), p.  
681 e1601360. doi: 10.1126/sciadv.1601360.
- 682 Thurfjell, H., Ciuti, S. and Boyce, M. S. (2014) ‘Applications of step-selection functions in  
683 ecology and conservation’, *Movement Ecology*, 2(1), pp. 1–12. doi: 10.1186/2051-3933-2-4.
- 684 Turner, W. *et al.* (2003) ‘Remote sensing for biodiversity science and conservation’, *Trends*  
685 *in Ecology & Evolution*. Elsevier Current Trends, 18(6), pp. 306–314. doi: 10.1016/S0169-  
686 5347(03)00070-3.
- 687 Wald, L. (1999) ‘Some terms of reference in data fusion’, *IEEE Transactions on Geoscience*  
688 *and Remote Sensing*, 37(3 I), pp. 1190–1193. doi: 10.1109/36.763269.
- 689 Williams, H. J. *et al.* (2020) ‘Optimizing the use of biologgers for movement ecology  
690 research’, *Journal of Animal Ecology*. Edited by J. Gaillard. Blackwell Publishing Ltd, 89(1),  
691 pp. 186–206. doi: 10.1111/1365-2656.13094.
- 692 Worton, B. J. (1989) ‘Kernel methods for estimating the utilization distribution in home-  
693 range studies’, *Ecology*, 70(1), pp. 164–168. doi: 10.2307/1938423.
- 694 Xie, Y., Sha, Z. and Yu, M. (2008) ‘Remote sensing imagery in vegetation mapping: a  
695 review’, *Journal of Plant Ecology*, 1(1), pp. 9–23. doi: 10.1093/jpe/rtm005.
- 696 Xue, J. and Su, B. (2017) ‘Significant Remote Sensing Vegetation Indices: A Review of  
697 Developments and Applications’, *Journal of Sensors*, 2017, pp. 1–17. doi:  
698 10.1155/2017/1353691.
- 699 Zhang, T., Ramakrishnan, R. and Livny, M. (1996) ‘BIRCH: An efficient clustering method  
700 for very large databases’, in *Proceedings of the 1996 ACM SIGMOD international conference*  
701 *on Management of data - SIGMOD ’96*. New York, New York, USA: ACM Press, pp. 103–  
702 114. doi: 10.1145/233269.233324.

703